β^+ Gamow-Teller Transition Strengths from ^{46}Ti and Stellar Electron-Capture Rates

S. Noji,[1,2,*] R. G. T. Zegers,[1,2,3] Sam M. Austin,[1,2,3] T. Baugher,[1,3] D. Bazin,[1] B. A. Brown,[1,3] C. M. Campbell,[4] A. L. Cole,[5] H. J. Doster,[1,3] A. Gade,[1,3] C. J. Guess,[6,7] S. Gupta,[8] G. W. Hitt,[9] C. Langer,[1,2] S. Lipschutz,[1,3] E. Lunderberg,[1,3] R. Meharchand,[10] Z. Meisel,[1,2,3] G. Perdikakis,[11,1] J. Pereira,[1] F. Recchia,[1] H. Schatz,[1,2,3] M. Scott,[1,3] S. R. Stroberg,[1,3] C. Sullivan,[1,2,3] L. Valdez,[1] C. Walz,[1] D. Weisshaar,[1] S. J. Williams,[1] and K. Wimmer[11,1]

[1]*National Superconducting Cyclotron Laboratory, Michigan State University, East Lansing, Michigan 48824, USA*
[2]*Joint Institute for Nuclear Astrophysics, Michigan State University, East Lansing, Michigan 48824, USA*
[3]*Department of Physics and Astronomy, Michigan State University, East Lansing, Michigan 48824, USA*
[4]*Lawrence Berkeley National Laboratory, Berkeley, California 94720, USA*
[5]*Physics Department, Kalamazoo College, Kalamazoo, Michigan 49006, USA*
[6]*Department of Physics and Applied Physics, University of Massachusetts Lowell, Lowell, Massachusetts 01854, USA*
[7]*Department of Physics and Astronomy, Rowan University, Glassboro, New Jersey 08028, USA*
[8]*Indian Institute of Technology Ropar, Nangal Road, Rupnagar, Punjab 140001, India*
[9]*Department of Applied Mathematics and Sciences, Khalifa University of Science, Technology, and Research, P.O. Box 127788 Abu Dhabi, UAE*
[10]*Neutron and Nuclear Science Group, Los Alamos National Laboratory, Los Alamos, New Mexico 87545, USA*
[11]*Department of Physics, Central Michigan University, Mt. Pleasant, Michigan 48859, USA*

(Received 5 April 2014; published 25 June 2014)

The Gamow-Teller strength in the β^+ direction to ^{46}Sc was extracted via the $^{46}\mathrm{Ti}(t, {}^3\mathrm{He} + \gamma)$ reaction at 115 MeV/u. The γ-ray coincidences served to precisely measure the very weak Gamow-Teller transition to a final state at 991 keV. Although this transition is weak, it is crucial for accurately estimating electron-capture rates in astrophysical scenarios with relatively low stellar densities and temperatures, such as presupernova stellar evolution. Shell-model calculations with different effective interactions in the *pf* shell-model space do not reproduce the experimental Gamow-Teller strengths, which is likely due to *sd*-shell admixtures. Calculations in the quasiparticle random phase approximation that are often used in astrophysical simulations also fail to reproduce the experimental Gamow-Teller strength distribution, leading to strongly overestimated electron-capture rates. Because reliable theoretical predictions of Gamow-Teller strengths are important for providing astrophysical electron-capture reaction rates for a broad set of nuclei in the lower *pf* shell, we conclude that further theoretical improvements are required to match astrophysical needs.

DOI: 10.1103/PhysRevLett.112.252501 PACS numbers: 23.40.-s, 25.55.Kr, 26.30.Jk, 27.40.+z

Introduction.—Electron-capture (EC) rates on nuclei are essential ingredients for the modeling of core-collapse and thermonuclear supernovæ (SNe) [1]. In addition, EC rates are important for the description of crustal heating [2] and cooling [3] processes in neutron stars. The estimation of EC rates requires detailed knowledge of Gamow-Teller (GT) transition strengths [B(GT)] in the β^+ direction, associated with the transfer of spin ($\Delta S = 1$), isospin ($\Delta T = 1$), and no orbital angular momentum ($\Delta L = 0$). ECs on a large number of nuclei, primarily with $40 \leq A \leq 120$, play a role in these astrophysical scenarios. Moreover, at the temperatures and densities present in stellar environments, transitions from excited states are often significant [4–8] in addition to those from ground states. Measuring even a sizable fraction of all relevant strengths is impossible, and therefore it is important to perform targeted experiments to validate and improve theoretical calculations. In this Letter, we report on an experiment aimed at extracting GT strengths from ^{46}Ti to ^{46}Sc to investigate concerns raised [9] about the ability of theory to accurately predict β^+ GT strengths for nuclei in the lower *pf* shell [with the neutron (N) and proton number (Z) just exceeding the magic number 20]. It is shown that leading configuration-interaction models in which the model space is truncated to excitations within the *pf* shell fail to reproduce the data. Calculations in the quasiparticle random phase approximation (QRPA), which are also frequently used for astrophysical purposes, fail to reproduce the data as well.

GT strengths can be measured in β-decay experiments, but they only provide access to a limited Q-value window. Therefore, charge-exchange (CE) reactions at intermediate energies ($\gtrsim$100 MeV/u), which can provide full B(GT) distributions on the basis of a well-established proportionality between the CE cross section at zero momentum transfer and B(GT) [10–12], have become the preferred method to test theoretical calculations. In Ref. [9], a systematic study was performed for 13 stable *pf*-shell nuclei with $45 \leq A \leq 64$ based on CE data from (n, p), $(d, {}^2\mathrm{He})$ and $(t, {}^3\mathrm{He})$ experiments. It was found that EC rates derived from experimental B(GT) values are generally

reproduced satisfactorily by shell-model (SM) calculations using the GXPF1A [13–15] and KB3G [16] interactions, whereas QRPA calculations in the framework of Ref. [17] (which are frequently used in astrophysical simulations) tend to significantly overestimate the experimental EC rates. On the basis of the case of ^{45}Sc, a specific concern about the ability of the SM calculations to reproduce transitions to low-lying states was raised [9] for nuclei in the lower *pf* shell ($A \sim 45$). Similar concerns were raised on the basis of a study of the GT strengths from ^{46}Ti in the β^- direction [18]. In Ref. [19], the investigations on the isotope shifts in calcium ($N = 20$) showed that substantial configuration mixing involving nucleons from the *sd* shell is present in these isotopes. Since such mixing is not considered in the SM calculations with the above-mentioned interactions, those calculations might have structural deficiencies, in particular for the lightest *pf*-shell nuclei. It is these transitions to low-lying states that are especially critical for ECs at low stellar temperatures and densities in pre-SN stars [20] and for the neutron-star crustal processes.

To gain better insight into the ability of the theoretical models to accurately represent GT strengths for nuclei in the lower *pf* shell, we measured the $B(\mathrm{GT})$ distribution in ^{46}Sc by the $^{46}\mathrm{Ti}(0^+, \mathrm{g.s.})(t, {}^3\mathrm{He} + \gamma)$ reaction. In addition to the above-mentioned importance for pre-SN stars, ^{46}Ti is also important as a potential heat source during crustal heating of neutron stars [2]: the lowest 1^+ state in ^{46}Sc resides at 991 keV. If populated significantly by EC, its decay would release $991/46 \approx 22$ keV/u, and would make EC on ^{46}Ti an important heat source.

The $(t, {}^3\mathrm{He})$ reaction has been used previously to extract $B(\mathrm{GT})$ values for a number of transitions. In this experiment, we improved the capability of identifying and locating GT transitions to the lowest-lying 1^+ state at 991 keV in ^{46}Sc by combining the $^{46}\mathrm{Ti}(t, {}^3\mathrm{He})$ measurement with a coincidence measurement of de-excitation γ rays from the ^{46}Sc residue. By selecting a specific excitation energy obtained in the $(t, {}^3\mathrm{He})$ measurement, γ decays can be studied without ambiguities related to indirect feeding from higher-lying states. The power of such a technique was also demonstrated in, e.g., $(\alpha, \alpha'\gamma)$ experiments [21,22].

The development of a technique that combines a medium-energy CE probe with high-precision γ detection is also critical for future experiments with unstable isotopes in which the CE experiments must be run in inverse kinematics. Energy resolutions from two-body kinematics alone are on the order of 1 MeV, and are significantly worse than those for experiments in forward kinematics [23–26]. With γ-ray detection, spectroscopic information with resolutions on the order of tens of keV is attainable.

Experiment.—A 150-pnA, 150-MeV/u beam of ^{16}O impinged on a 3525-mg/cm^2-thick Be target. Tritons were selected from other reaction products using the A1900 fragment separator [27] with a 195-mg/cm^2-thick Al degrader [28]. The resulting triton beam (with rate ~5 Mpps, purity $> 99\%$, and average energy 115 MeV/u) was transported by using the dispersion-matching ion optics to a 10-mg/cm^2-thick and 77.1% isotopically enriched ^{46}Ti reaction target. The main contaminants were ^{48}Ti (17.3%) and ^{47,49,50}Ti (2.3%, 1.5%, and, 1.8%, respectively). A polyethylene (CH_2) target with a thickness of 10 mg/cm^2 was used for calibration purposes. ^{3}He reaction products were momentum analyzed by the S800 magnetic spectrometer [29], and detected at the focal plane by two cathode-readout drift chambers (CRDCs) [30] and a 5-mm-thick plastic scintillator. The CRDC data were used to reconstruct angles and momenta of the ^{3}He particles at the target. Excitation energies of ^{46}Sc over the range $0 \leq E_x \lesssim 20$ MeV with a resolution of 0.3 MeV(FWHM) were obtained in a missing-mass calculation. Scattering angles were measured over the range $0^\circ \leq \theta \lesssim 6^\circ$ with a resolution of 1.0°(FWHM).

The γ-ray detection system GRETINA [31], installed surrounding the reaction target, was used to measure the de-excitation γ rays from the ^{46}Sc residues. The use of this high-purity germanium detector was important as it allowed precise determination of γ-ray energies. The large peak-to-total ratio enabled a measurement of the very weak GT transition with a reasonable photopeak detection efficiency.

Results and analysis.—The double-differential cross sections for the $^{46}\mathrm{Ti}(t, {}^3\mathrm{He})$ reaction are shown in the left panel of Fig. 1. The systematic uncertainty of the absolute normalization of the cross section was estimated to be 6%.

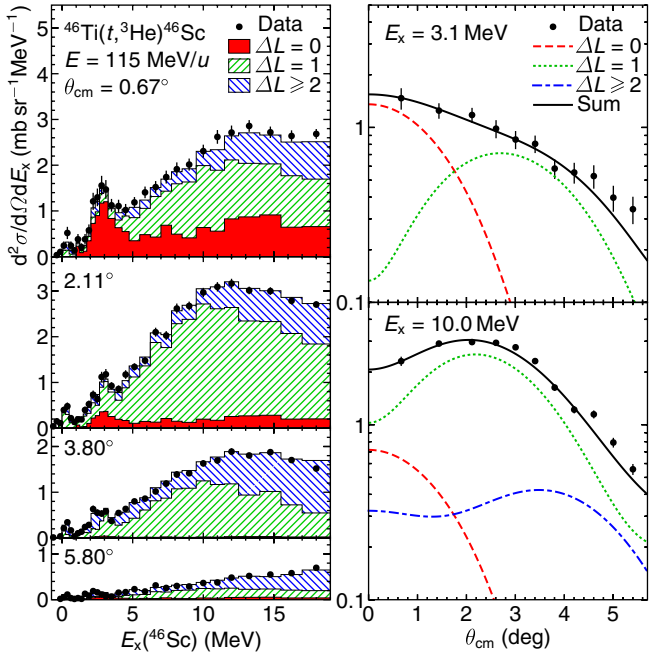

FIG. 1 (color online). (Left) Double-differential cross sections for the $^{46}\mathrm{Ti}(t, {}^3\mathrm{He})^{46}$Sc reaction at various scattering angles. The error bars denote the statistical uncertainty only. The histograms show the results from the MDA. (Right) Representative angular distributions for $E_x = 3.1$ and 10.0 MeV including the results from the MDA.

It was dominated by the uncertainty in the t-beam intensity, which was monitored by calibrating the current readout for the unreacted beam in a Faraday bar placed in the first dipole magnet of the A1900 against the well-known cross section for the $^{12}C(t,{}^3He)^{12}B(1^+,\text{g.s.})$ reaction [32].

A multipole decomposition analysis (MDA) [33,34] was performed for extracting the $\Delta L = 0$ (GT) component of the cross section. In this analysis, the angular distribution in each energy bin in $E_x(^{46}Sc)$ was fitted with a linear combination of angular distributions calculated in the distorted-wave Born approximation (DWBA) with $\Delta L = 0$, 1, 2, and 3. The calculations were performed with the microscopic, double-folding DWBA code FOLD/DWHI [35]. The single-particle wave functions for t and ^{3}He were taken from variational Monte Carlo calculations [36], and those for ^{46}Ti and ^{46}Sc were generated by using a Woods-Saxon potential. One-body transition densities were calculated following the description in Ref. [37]. The Love-Franey effective NN interaction at 140 MeV [38] was used. Optical model potential (OMP) parameters were taken from those for ^{3}He + ^{58}Ni at 443 MeV in Ref. [39], and compared with calculations based on OMP parameters from Ref. [40] to estimate systematic uncertainties.

Results from MDA are included in the left panel of Fig. 1. As shown, the angular distributions are well reproduced by MDA. It can be seen that the $\Delta L = 0$ component is consistent with zero around the ground state, with a broad peak at around 3 MeV. Systematic errors due to the choice of the OMP parameters and the choice of multipole components were estimated to be 5% by performing several trials with different sets of reasonable input parameters.

The $B(\text{GT})$ was determined from the extracted $\Delta L = 0$ cross sections by using the proportionality relation [10–12] between the $\Delta L = 0$ cross section at 0°, $\sigma_{\Delta L=0}(0°)$, and $B(\text{GT})$,

$$\sigma_{\Delta L=0}(0°) = \hat{\sigma}_{\text{GT}} F(q,\omega) B(\text{GT}),$$

where $\hat{\sigma}_{\text{GT}}$ is the GT unit cross section and $F(q,\omega)$ is a kinematical correction factor representing the dependence of $\sigma_{\Delta L=0}(0°)$ on the momentum (q) and the energy (ω) transfers. Unit cross sections for the $(t,{}^3\text{He})$ and $({}^3\text{He},t)$ reactions at this energy follow $\hat{\sigma}_{\text{GT}} = 109/A^{0.65}$ [12], with A being the mass number of the target nucleus. The value $\hat{\sigma}_{\text{GT}}|_{A=46} = 9.05$ mb/sr was used for the present analysis. The extracted $B(\text{GT})$ distribution is shown in Fig. 2. The contribution from the ^{48}Ti contamination in the reaction target was subtracted based on the $B(\text{GT})$ values extracted from existing $^{48}\text{Ti}(d,{}^2\text{He})$ data [41,42] up to $E_x(^{48}Sc) = 5$ MeV, which corresponds to $E_x(^{46}Sc) = 6.6$ MeV with the Q-value difference of 1.6 MeV taken into account. The systematic uncertainty due to this subtraction process is less than 5%.

More detailed information on the low-lying states is provided by studying the decay by γ emission. Figure 3(a) shows a plot of the γ-ray energy (E_γ) measured in GRETINA and the excitation energy $E_x(^{46}Sc)$ determined from the $(t,{}^3\text{He})$ data. The near absence of events for which $E_\gamma > E_x$ indicates that background was nearly nonexistent. The clear drop of the the γ-ray yield at the proton and neutron separation energies ($S_p = 8235.1$ keV and $S_n = 8760.62$ keV) is observed. The lowest known 1^+ state is at 991 keV, which decays to the 444-keV 2^+ state with a 100% branching emitting a 547-keV γ ray [see Ref. [43] and the schematic decay diagram in the inset in Fig. 3(b)]. Figure 3(b) is a γ-ray energy spectrum gated on $E_x = 991 \pm 380$ keV in the $^{46}\text{Ti}(t,{}^3\text{He})$ excitation energy spectrum, where the width of the gate corresponds to 3σ of the excitation energy resolution. Since other states that are

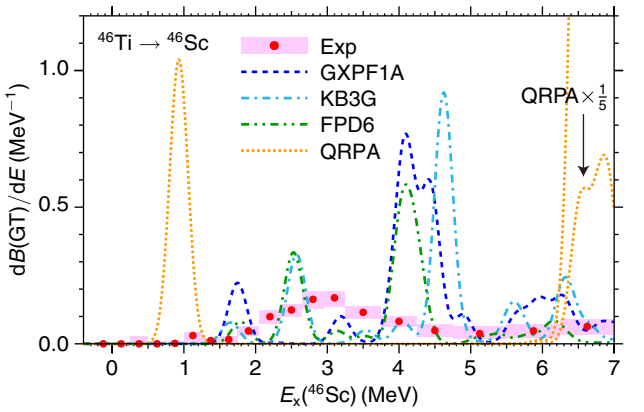

FIG. 2 (color online). $B(\text{GT})$ distribution extracted in the MDA of the $^{46}\text{Ti}(t,{}^3\text{He})$ data. The error bars denote the statistical and systematic uncertainties. The theoretical calculations are also shown.

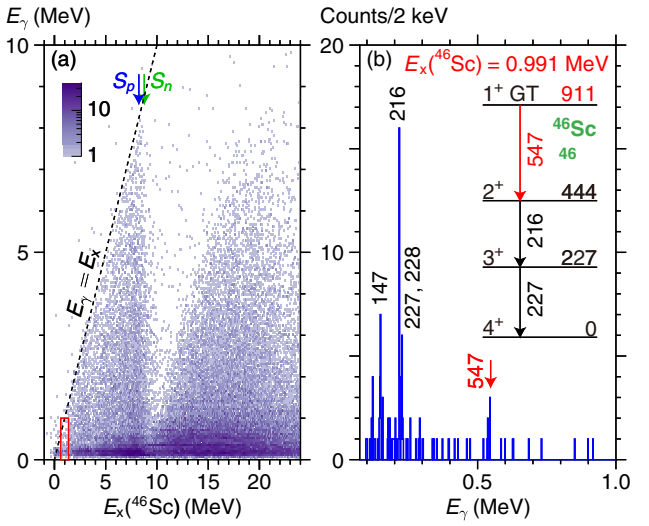

FIG. 3 (color online). (a) E_γ versus $E_x(^{46}Sc)$. The $E_\gamma = E_x$ line is shown, and the proton (S_p) and neutron (S_n) separation energies are also indicated. (b) A projection of (a) onto the E_γ axis, gated on $E_x(^{46}Sc)$ around 991 keV as indicated by the box in (a). The inset shows a schematic decay diagram of the 1^+ state at 991 keV.

potentially excited and that are contained in this gate do not decay through the 991-keV state, the observation of events with the 547-keV γ ray in Fig. 3(b) directly relates to the excitation of the 1^+ state at 991 keV. Other distinct lines are seen at $E_\gamma = 147$, 216 and 227 keV.

The yield for the 547-keV γ rays can be converted to a $B(\mathrm{GT})$ for the excitation of the 991-keV state after taking into account the detection efficiency of GRETINA. The obtained $B(\mathrm{GT})$ of this state was $0.009 \pm 0.005(\mathrm{exp.}) \pm 0.003(\mathrm{tensor})$. The error labeled "exp." is the sum of statistical and the experimental systematic contributions. The error labeled "tensor" indicates the estimated uncertainty [44,45] due to interference effects between $\Delta L = 0$, $\Delta S = 1$ and $\Delta L = 2$, $\Delta S = 1$ amplitudes mediated via the tensor interaction [10]. This effect can be relatively strong for very weak Gamow-Teller transitions such as this one. It would have been impossible to determine such a weak GT transition, which is critical for the calculation of EC rates (see below), with the data from the $^{46}\mathrm{Ti}(t, {}^3\mathrm{He})$ reaction alone.

Comparison with theory.—The $B(\mathrm{GT})$ distributions from the experiment and theoretical calculations (convoluted with the experimental resolution) are compared in Fig. 2. The SM calculations [46] were performed in the full *pf* shell-model space with the GXPF1A, KB3G, and FPD6 [47] interactions by using an effective operator $(\sigma\tau_+)_{\mathrm{eff}} = 0.744\sigma\tau_+$ [48]. None of the SM calculations agree well with the data: the bump at ~3 MeV in the experimental distribution is not reproduced, and the strong peaks in the SM calculations at 4–5 MeV are not observed in the experiment. In addition, none of the SM calculations predict a weak transition to a state at ~1 MeV. Also shown is the $B(\mathrm{GT})$ distribution based on the QRPA calculation mentioned above. It predicts the lowest-lying state at 930 keV, close to the experimentally observed energy, but with a $B(\mathrm{GT})$ of 0.34, almost 40 times larger than observed. In addition, the next 1^+ state does not appear until 6 MeV.

Intruder states relative to the *pf*-shell configurations are important for nuclei in the lower part of the *pf* shell. The configuration of these intruder states involves nucleons excited from the *sd* shell into the *pf* shell. The lowest-lying levels that cannot be described by the *pf* shell include the 1.84-MeV 0^+ state in ^{42}Ca, the 0.15-MeV $3/2^+$ state in ^{43}Sc, the 0.01-MeV $3/2^+$ state in ^{45}Sc, and the 2.61-MeV 0^+ state in ^{46}Ti. The mixing with intruder states is known to be necessary to describe the large 2^+ to 0^+ $B(\mathrm{E2})$ values for ^{42,44}Ca (see Fig. 13 of Ref. [14]). The Hamiltonians we use treat these intruder states in different ways. FPD6 was derived only from nuclei in the lower part of the *pf* shell, $^{44-49}$Ca, $^{42-44}$Sc, and ^{44}Ti. As such FPD6 is highly influenced by the intruders. On the other hand, GXPF1A was obtained for nuclei with $A \geq 47$ in order to minimize the influence of intruder states. A difference in these Hamiltonians shows up as the summed GT strength up to 7 MeV with ratios to experiment of 1.8 (GXPF1A) and 1.1 (FPD6). Thus, it appears that the influence from intruder states can be partially accounted for by the effective Hamiltonian. The Hamiltonian sensitivity for the summed strength can be traced to the the $p_{3/2}$–$f_{7/2}$ single-particle energy gap being 2.94 MeV with GXPF1A to 1.89 MeV with FPD6. However, the details of the $B(\mathrm{GT})$ distribution are poorly described even with FPD6. It is likely that the intruder states will need to be explicitly included in the calculations. We also note that the discrepancies between experiment and theory are significantly stronger than those observed for the GT transitions from ^{46}Ti in the β^- direction [18]. It will be a challenge for future calculations to explicitly include these intruder configurations in order to consistently describe all of the observations in this mass region, including the energies of the low-lying states, the $B(\mathrm{E2})$ values, and our observed $B(\mathrm{GT})$ distribution.

Electron-capture rates.—In Fig. 4, EC rates (λ_{EC}) based on the experimental and theoretical GT strength distributions are compared. The calculations are as described in Ref. [9] and follow the formalism of Refs. [4–7], implemented in a code previously used in Refs. [2,9]. In the present calculations we only considered transitions from the ground state of the parent nucleus. Since nuclei in the lower *pf* shell such as ^{46}Ti are particularly important during the pre-SN evolution of massive stars [20], we present the rates at an electron density $\rho Y_{\mathrm{e}} = 10^7$ g/cm^3 and in a temperature range $2.5 < T/10^9\ \mathrm{K} < 4.5$ of relevance for that phase. Under these conditions, ECs into low-lying 1^+ states dominate the total rate. Even though this state is associated with a very small GT strength, this EC rate dominates except at the higher temperatures. Of the different SM interactions, the EC rate based on the GXPF1A interaction is the closest to that based on the data, but we note that this is coincidental given the poorer overall

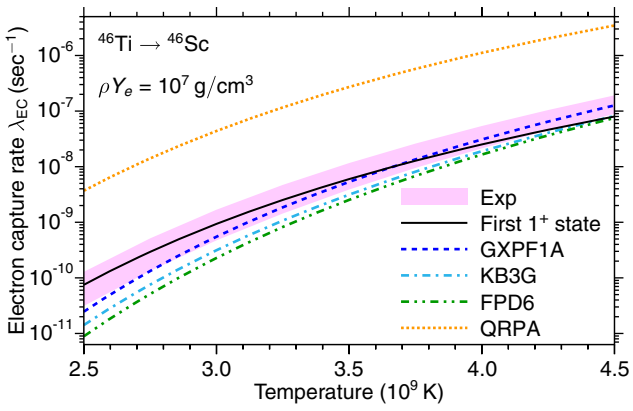

FIG. 4 (color online). EC rates on ^{46}Ti. The shaded band denotes the EC rate based on the experimental GT strengths (including uncertainties), whereas the solid line only represents the EC into the 1^+ state at 991 keV. The total rates based on the theoretical calculations are also shown.

description of the data by this interaction. The EC rate based on the QRPA calculation significantly overestimates (by about a factor of 40) the EC rate based on the data, basically reflecting the overestimated $B(\mathrm{GT})$ for the low-lying excitation.

Summary.—The GT strength distribution in ^{46}Sc was extracted from $^{46}\mathrm{Ti}(t, {}^3\mathrm{He}+\gamma)$ data, and coincidences with γ rays associated with the de-excitation of ^{46}Sc were used to extract the otherwise inaccessible GT strength for the excitation of the 1^+ state at $E_x(^{46}\mathrm{Sc}) = 991$ keV. Significant deficiencies in SM calculations based on the GXPF1A, KB3G, and FPD6 interactions for the *pf* shell were observed, likely due to admixtures from *sd*-shell configurations which are not included in the calculations. QRPA calculations used for astrophysical modeling of EC rates also poorly reproduce the experimental GT strengths. We conclude that further improvements to theoretical calculations of GT strengths for nuclei in the lower *pf* shell are important, as derived EC rates for these nuclei at relevant astrophysical densities and temperatures are especially sensitive to the detailed structure of excitations to low-lying states. CE experiments at intermediate energies in combination with high-resolution γ-ray detection will be of significant use to benchmark improved theoretical descriptions, in particular for experiments in inverse kinematics with unstable isotope beams at present and future rare isotope beam facilities.

We thank all the staff at NSCL for their support. This work was supported by the US NSF grant PHY-08-22648 (Joint Institute for Nuclear Astrophysics) and PHY-10-68217. GRETINA was funded by the US DOE Office of Science. Operation of the array at NSCL is supported by NSF under Cooperative Agreement PHY-11-02511 (NSCL) and DOE under grant DE-AC02-05CH11231 (LBNL).

*noji@nscl.msu.edu

[1] K. Langanke and G. Martínez-Pinedo, Rev. Mod. Phys. **75**, 819 (2003).
[2] S. Gupta, E. F. Brown, H. Schatz, P. Möller, and K.-L. Kratz, Astrophys. J. **662**, 1188 (2007).
[3] H. Schatz *et al.*, Nature (London) **505**, 62 (2014).
[4] G. M. Fuller, W. A. Fowler, and M. J. Newman, Astrophys. J. Suppl. Ser. **42**, 447 (1980).
[5] G. M. Fuller, W. A. Fowler, and M. J. Newman, Astrophys. J. **252**, 715 (1982).
[6] G. M. Fuller, W. A. Fowler, and M. J. Newman, Astrophys. J. Suppl. Ser. **48**, 279 (1982).
[7] G. M. Fuller, W. A. Fowler, and M. J. Newman, Astrophys. J. **293**, 1 (1985).
[8] K. Langanke and G. Martínez-Pinedo, Nucl. Phys. **A673**, 481 (2000).
[9] A. L. Cole, T. S. Anderson, R. G. T. Zegers, Sam M. Austin, B. A. Brown, L. Valdez, S. Gupta, G. W. Hitt, and O. Fawwaz, Phys. Rev. C **86**, 015809 (2012).
[10] T. N. Taddeucci, C. A. Goulding, T. A. Carey, R. C. Byrd, C. D. Goodman, C. Gaarde, J. Larsen, D. Horen, J. Rapaport, and E. Sugarbaker, Nucl. Phys. **A469**, 125 (1987).
[11] R. G. T. Zegers *et al.*, Phys. Rev. Lett. **99**, 202501 (2007).
[12] G. Perdikakis *et al.*, Phys. Rev. C **83**, 054614 (2011).
[13] M. Honma, T. Otsuka, B. A. Brown, and T. Mizusaki, Phys. Rev. C **65**, 061301(R) (2002).
[14] M. Honma, T. Otsuka, B. A. Brown, and T. Mizusaki, Phys. Rev. C **69**, 034335 (2004).
[15] M. Honma, T. Otsuka, B. A. Brown, and T. Mizusaki, Eur. Phys. J. A **25**, 499 (2005).
[16] A. Poves, J. Sánchez-Solano, E. Caurier, and F. Nowacki, Nucl. Phys. **A694**, 157 (2001).
[17] P. Möller and J. Randrup, Nucl. Phys. **A514**, 1 (1990).
[18] T. Adachi *et al.*, Phys. Rev. C **73**, 024311 (2006).
[19] E. Caurier, K. Langanke, G. Martínez-Pinedo, F. Nowacki, and P. Vogel, Phys. Lett. B **522**, 240 (2001).
[20] A. Heger, S. E. Woosley, G. Martínez-Pinedo, and K. Langanke, Astrophys. J. **560**, 307 (2001).
[21] D. Savran, M. Babilon, A. M. van den Berg, M. N. Harakeh, J. Hasper, A. Matic, H. J. Wörtche, and A. Zilges, Phys. Rev. Lett. **97**, 172502 (2006).
[22] D. Savran, A. M. van den Berg, M. N. Harakeh, K. Ramspeck, H. J. Wörtche, and A. Zilges, Nucl. Instrum. Methods Phys. Res., Sect. A **564**, 267 (2006).
[23] R. G. T. Zegers *et al.*, Phys. Rev. Lett. **104**, 212504 (2010).
[24] M. Sasano *et al.*, Phys. Rev. Lett. **107**, 202501 (2011).
[25] M. Sasano *et al.*, Phys. Rev. C **86**, 034324 (2012).
[26] R. Meharchand *et al.*, Phys. Rev. Lett. **108**, 122501 (2012).
[27] D. J. Morrissey, B. M. Sherrill, M. Steiner, A. Stolz, and I. Wiedenhoever, Nucl. Instrum. Methods Phys. Res., Sect. B **204**, 90 (2003).
[28] G. W. Hitt *et al.*, Nucl. Instrum. Methods Phys. Res., Sect. A **566**, 264 (2006).
[29] D. Bazin, J. A. Caggiano, B. M. Sherrill, J. Yurkon, and A. Zeller, Nucl. Instrum. Methods Phys. Res., Sect. B **204**, 629 (2003).
[30] J. Yurkon, D. Bazin, W. Benenson, D. J. Morrissey, B. M. Sherrill, D. Swan, and R. Swanson, Nucl. Instrum. Methods Phys. Res., Sect. A **422**, 291 (1999).
[31] S. Paschalis *et al.*, Nucl. Instrum. Methods Phys. Res., Sect. A **709**, 44 (2013).
[32] C. J. Guess *et al.*, Phys. Rev. C **80**, 024305 (2009).
[33] B. Bonin *et al.*, Nucl. Phys. **A430**, 349 (1984).
[34] M. Ichimura, H. Sakai, and T. Wakasa, Prog. Part. Nucl. Phys. **56**, 446 (2006).
[35] J. Cook and J. Carr, computer program FOLD/DWHI, Florida State University (unpublished); based on F. Petrovich and D. Stanley, Nucl. Phys. **A275**, 487 (1977); modified as described in J. Cook, K. W. Kemper, P. V. Drumm, L. K. Fifield, M. A. C. Hotchkis, T. R. Ophel, and C. L. Woods, Phys. Rev. C **30**, 1538 (1984); R. G. T. Zegers, S. Fracasso, and G. Colò (unpublished).
[36] S. C. Pieper and R. B. Wiringa, Annu. Rev. Nucl. Part. Sci. **51**, 53 (2001).
[37] K. Yako *et al.*, Phys. Rev. Lett. **103**, 012503 (2009).
[38] M. A. Franey and W. G. Love, Phys. Rev. C **31**, 488 (1985).
[39] J. Kamiya *et al.*, Phys. Rev. C **67**, 064612 (2003).

[40] T. Furumoto, Y. Sakuragi, and Y. Yamamoto, Phys. Rev. C **82**, 044612 (2010).
[41] S. Rakers *et al.*, Phys. Rev. C **70**, 054302 (2004).
[42] E.-W. Grewe *et al.*, Phys. Rev. C **76**, 054307 (2007).
[43] S.-C. Wu, Nucl. Data Sheets **91**, 1 (2000).
[44] R. G. T. Zegers *et al.*, Phys. Rev. C **74**, 024309 (2006).
[45] G. W. Hitt *et al.*, Phys. Rev. C **80**, 014313 (2009).
[46] B. A. Brown, W. D. M. Rae, E. McDonald, and M. Horoi, NuShellX@MSU, http://www.nscl.msu.edu/~brown/resources/resources.html.
[47] W. A. Richter, M. G. Van Der Merwe, R. E. Julies, and B. A. Brown, Nucl. Phys. **A523**, 325 (1991).
[48] G. Martínez-Pinedo, A. Poves, E. Caurier, and A. P. Zuker, Phys. Rev. C **53**, R2602(R) (1996).